Journal of Engineering Science and Technology
Vol. 12, No. 11 (2017) 2965 - 2989

ALIVE-IN-RANGE MEDIUM ACCESS CONTROL PROTOCOL TO MINIMIZE DELAY IN UNDERWATER WIRELESS SENSOR NETWORK COMMUNICATION AT A FREQUENCY OF 2.4 GHz

VIKAS RAINA*, MANISH KUMAR JHA,
PARTHA PRATIM BHATTACHARYA

Department of ECE, CET, Mody University of Science and Technology,
Lakshmangarh, Sikar, Rajasthan, 332311, India
*Corresponding Author: vikasraina.raina04@gmail.com

Abstract

Time synchronization between the sensor nodes to reduce end to end delay for critical and real time data monitoring can be achieved by cautiously monitoring the mobility of the mobile sink node in underwater wireless sensor networks. The proposed Alive-in-Range (AR-MAC) medium access control protocol monitors delay sensitive, critical and real time data. The idea evolves as a reduction in duty cycle, precise time scheduling of active/sleep cycles of the sensors, monitoring the mobility of the sink node along-with the selection of appropriate queues and schedulers can reduce the end to end delay enhancing other performance metrics too. The algorithms effective path determination and optimum throughput path determination are proposed. It is assumed that the sensors are properly anchored to limit their movement due to waves within the permissible limits to follow these algorithms. This paper attempts to utilize electromagnetic waves at resonance frequency of 2.4 GHz for underwater communication. The results verify that the implementation of Alive-in-Range MAC protocol has reduced the average end to end delay significantly making it appropriate for critical and real time data monitoring. This work proves the suitability of electromagnetic waves as an effective alternative for underwater wireless communication. The main objective is to mitigate sink neighbourhood problem, distance constrained mobile sink problem and to reduce the average end to end delay by implementing Alive-in-Range (AR-MAC) medium access control protocol in underwater sensor networks and to draw the attention of researchers in this area.

Keywords: Underwater wireless sensor network, Mobile sink, Queue, Scheduler, Alive-in-Range MAC, Effective path determination, Optimum throughput path determination.

Nomenclatures

B	The bandwidth, Hertz
D	The relative deadline, seconds
G	*The gain of an antenna, dBm*
g	The channel gain, dBm
K	The ratio of data rate of transmission to the message length
l	The length of a message, bytes
m, n	The curve fitting coefficients
P	The priority of a task
PD	The probability of successful data transmission
Q	The service time, seconds
R	*The required number of time slots*
r	The rate of data generation, bps
T	The period of inter arrival time, seconds
T_{sim}	Total simulation time of the network, seconds
X	The number of packets present in the system

Greek Symbols

α	The attenuation constant
β	The phase shifting constant
δ	The average end to end delay, seconds
ε_r	The relative permittivity
ε_t	The tangent loss, dBm
Θ	The value of loss, dBm
κ	The size of payload, bytes
λ	The wavelength, m
$\mathcal{P}$	The desired position of the sink
ρ	The throughput, bps
Ψ	The value of power, dBm
Π	An arbitrary packet
$\hbar$	The reference throughput, bps

Abbreviations

AR-MAC	Alive-in-Range Medium Access Control
AUV	Autonomous Underwater Vehicle
EM	Electromagnetic
FFD	Full Function Device
IFS	Inter Frame Sequence
LIFS	Long Inter Frame Sequence
MAC	Medium Access Control
MILP	Mixed Integer Linear Programming
MPDU	Medium Access Control Protocol Data Unit
RFD	Reduce Function Device
SIFS	Short Inter Frame Sequence
TDMA	Time Division Multiple Access
UWSN	Underwater Wireless Sensor Network

1. Introduction

Recently, unmanned underwater explorations have gained interest in monitoring aquatic environs (comprising ponds, lakes, rivers, oceans and reservoirs, etc.) for commercial utilization, scientific investigation and disaster prevention. An exemplary system for such type of extensive monitoring is a network constitute of hundreds of tiny autonomous wireless sensors and vehicles distributed underwater communicating with each other using wireless link, performing collaborative tasks known as underwater wireless sensor networks. They augment our ability to observe and predict the aqueous environments by enabling many applications such as tactical surveillance, assisted navigation, disaster prevention, oceanographic data collection, pollution monitoring and offshore exploration [1]. Although in the specific applications including critical and real time data monitoring for limited time period, such as rescue operations and military operations of importance of national security, the parameters like throughput, end to end delay, jitter and packets dropped are highly influential. These time-bounded operations also have strict deadlines to save lives, infrastructures and resources. As the available battery power with already deployed sensor nodes cannot be increased, but the battery power of sensor nodes intentionally deployed for the operation and petrol/electricity in the autonomous underwater vehicles (AUVs) can be adjusted according to the tentative duration of the operations.

The life-threatening rescue operations during Tsunamis, sinking of a ship/boat, failure of oxygen generation plant in submarines and sinking of submarines due to technical malfunctioning require highly efficient data collection techniques with permissible delay and minimum data loss for gathering meaningful and useful information. The continuous monitoring of underwater parameters closer to the rescue team (sink) and location of the rescue vehicle throughout the operation is highly desirable for the successful execution of the operation. The low and distance-dependent bandwidth, high latency, floating node mobility, sparse deployment, high error probability, frequency dependent transmission range, 3-dimensional space and poor channel conditions lead to larger power consumption on transmissions and thus multi-hop transmissions are not always attractive in underwater communication [1]. Therefore, the proposed AR-MAC protocol is capable of continuous monitoring of critical underwater events in a very cost effective manner, as it utilizes relatively low-cost, reduced function devices (RFDs) only in the network avoiding multi-hop transmissions.

2. Related Work

This section introduces the related work as many researchers are working in this field of research. Akyildiz et al. [1-2] recognize research challenges, mainly focusing on protocol issues, hardware issues and a cross-layer design approach for UWSNs. The elemental technology used in the physical layer of underwater acoustic sensor networks is acoustic communication, as optical signals and electromagnetic signals are unsuited due to high absorption, scattering and attenuation, respectively, in the aqueous environments. They are different from terrestrial sensor networks in many attitudes: 3-dimensional space, frequency dependent transmission range, floating node mobility, longer delay, low and distance dependent bandwidth, and many more. The propagation velocity of the acoustic waves underwater is approximately 1500 m/s and the available

bandwidth at a few kilometers is of the order of 10 kHz [2]. Liang et al. [3] proposed controlled mobile sink approach in wireless sensor networks (WSNs) to prolong the network lifetime. The least amount of time at each sojourn location of the mobile sink is calculated to minimize the packet loss and the problem is formulated as a mixed integer linear programming (MILP). The results showed the enhancement in network lifetimes, provided by various algorithms by varying the (i) value of the total distance travel per tour L from 350 to 525 meters while keeping maximum range between two sojourns R_{max}= 35 m and the least sojourn time at each location T_{min} = 600 seconds to be fixed (ii) by varying R_{max} from 0 to 100 meters while keeping L = 400 m and T_{min} = 600 seconds to be fixed (iii) by varying the value of T_{min} from 0 to 5000 seconds while keeping R_{max} = 400 m and the L = 35 m to be fixed.

In Ayaz et al. [4] a thorough evaluation and comparison of different routing techniques for UWSNs is given. A typical geographical routing protocol vector-based forwarding is implemented in [5] and the performance of delay tolerant network routing protocol for underwater sensor networks is evaluated in [6]. Autonomous underwater vehicle aided routing for underwater sensor networks is discussed in [7-8]. Quality of service ability with polling-based scheduling for wireless body sensor networks is presented in [9]. Konstantopoulos et al. [10] investigated a rendezvous based approach with mobile sinks. Many mobile sink trajectories are implemented in [11-13]. The current state-of-the-art solutions in underwater delay tolerant networks are proposed in [14]. A survey of data collection in WSNs with mobile elements has been done in [15]. Kartha et al. [16] have compared analytical models for delay performance to observe that the polling model is more effective in modelling the mobility-assisted data collection framework for UWSNs. The implemented analytical models are validated with the experimental setup developed using the NS-2 based AquaSim simulator. The outcomes illustrate that the proposed framework reveals superior performance in terms of energy efficiency, network lifetime and packet delivery ratio at the cost of increased message latency.

In 2013, Sendra et al. [17] have performed a set of measurements of electromagnetic (EM) waves at 2.4 GHz in underwater environments. The water conditions are fixed and the behavior of EM waves as a function of several network parameters such as the working frequency, data transfer rates and modulations are analyzed. The output data rates are calculated at different frequencies and distances.

Elrashidi et al. [18] presented a comprehensive study of electromagnetic waves underwater propagation for a wireless sensor network at a resonance frequency of 2.4 GHz. A mathematical model for the path loss due to attenuation of electromagnetic waves in sea and pure water is introduced. A bow tie antenna is used for high gain to compensate the high path loss. A reflection model is introduced to illustrate the impact of air-water and water-sand interfaces as a function of distance between sensors and water depth. The path loss is evaluated and compared as a function of resonance frequency at different distances between the sensors for pure and sea water. A high gain bow tie antenna is designed and results such as radiation patterns, return loss, voltage standing wave ratio, input impedance and antenna gain at 2.4 GHz is calculated.

Letre et al. [19] performed the analysis of throughput and delay of unslotted IEEE 802.15.4 protocol as it is a protocol offering high reliability as a low power and low data rate protocol. The maximum throughput and minimum delay of the unslotted version of the protocol is analysed at the frequency of 2.4 GHz. The maximum throughput and minimum delay are calculated at different operating frequencies and at various address sizes. Finally, the comparison of the bandwidth efficiency for 2.4 GHz and 868/915 MHz is performed and the minimum delay as a function of payload size at the frequency of 2.4 GHz is evaluated.

Yu et al. [20] have introduced a low jitter scheduling technique clarifying the dependence of TDMA scheduling for sensors and point out the correlations between the scheduling delays, overall quality control and focus on reducing jitter in scheduling. The values of normalized jitter at starting and ending time slots are evaluated.

Aoun et al. [21] consider the problem of modelling the transmission of real time data from a single node of a wireless sensor network to the next hop or access point. A thresholding policy is introduced that is supported by an analytical model and it is responsible for deciding whether to transmit a data packet or drop it and transmit the next one. A sensor system model, packet delivery ratio calculation and probability of an empty system are introduced. The packet delivery ratio gain with respect to the packet arrival rate is evaluated.

Liu et al. [22] have introduced a Doppler assisted time synchronization scheme for mobile underwater wireless sensor networks. The Doppler scaling factor is estimated to gather relative movement velocities of sensor nodes. A model is developed to establish a relationship between the joint and individual Doppler Effect caused by the sensor mobility and clock skew. The synchronization, data collection, velocity estimation, propagation delay estimation and linear regression phases are thoroughly analysed. The propagation delay with respect to velocity and clock skew is estimated. The evaluation of error versus time after synchronization, calculation of energy with varying error tolerance and improvement by calibration at a particular value of a clock skew is performed.

Yang et al. [23] exploit mobility of the sink node to transmit non delay-sensitive data and avoid multi-hop transmissions. An area partitioning algorithm, a transmission mechanism based on superposition coding and a MAC protocol has been proposed. The simulation results produce optimum values of minimum distance algorithm and maximum throughput algorithm with respect to traveling distance (m), transmission throughput (bps), time spent in each group (secs) and energy consumption of the group (Joule) at the different number of the sensor nodes.

The major contributions of this paper are as follows. It refers the sink neighbourhood problem and the distance-constrained mobile sink problem. A new methodology has been developed which utilizes the sink node velocity, most suitable path with controlled mobility, low duty cycle, appropriate number of queues having optimum queue length, proper schedulers and finally the AR-MAC protocol has been implemented to improve the network performance.

The rest of the paper is organized as follows. The related work is presented in section 2. Section 3 illustrates the proposed AR-MAC protocol. Section 4 presents preliminaries. The mathematical models are explained in section 5. Section 6

constitutes of explanation of simulation scenarios and algorithms. Section 7 illustrates simulation results and analysis. Section 8 concludes the paper and presents the future work.

3. The Proposed Alive-in-Range MAC (AR-MAC) Protocol

In AR-MAC as the sink node is continually mobile without sojourns, a centralized duty-cycle based MAC protocol is used to schedule the transmissions from the sensors. Normally, all the sensor nodes are in the sleep state. As the sink traverses a most effective path, the sensors coming into the range of sink node become active and start transmissions. The maximum range of data transmission is 20 meters. It is determined with respect to the effective received power at the sink node. For example, as shown in Fig. 1 when the mobile sink node is at location 1, the sensor nodes A and B are in its range. After the sink moves into the range, the sensor nodes A and C become active after sensing the beacons. At location 2 and 3, the sensors A, B, C and D are in range and become active. At position 4, the sensor nodes A and C are out of range and enter the sleep mode, but nodes B and D are still in active mode. The centralized approach to schedule active cycles eliminates collisions and also reduces the synchronization requirements among the sensors. Figure 2 presents the timing diagram of active/sleep scheduling. The process of data transmission and data reception of the proposed AR-MAC protocol with two sensors is shown in Fig. 3. It illustrates that, after the sink moves to the data collection position, it polls each sensor sequentially. A sensor with data to transmit does so immediately after it is polled and in the absence of data, sends a small packet to just acknowledge the receipt of the poll. Then the sink estimates the propagation delay for each sensor based on the measurement of the round trip time. A sensor may be re-polled immediately if its data is not received correctly. Also, if no response is obtained in response to a poll, the sink may repeat polls subject to limit the number of retransmissions. After the uplink transmissions, the sink transmits the control messages to the sensors. The messages sent by the sink also contain the schedule according to which the sensors send back their acknowledgement packets (ACK).

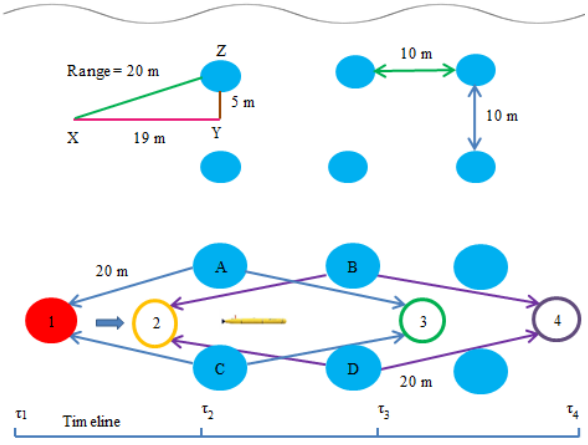

Fig. 1. The simulation architecture of the proposed AR-MAC protocol.

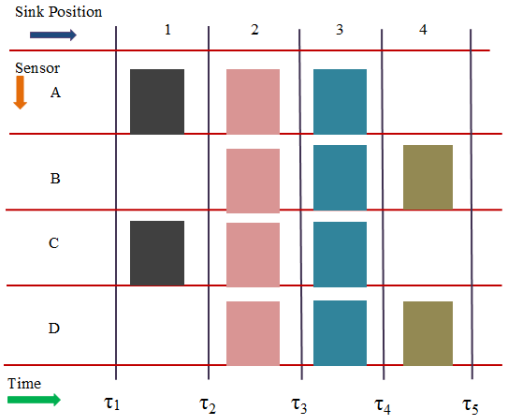

Fig. 2. The timing diagram of active and sleep scheduling in AR-MAC.

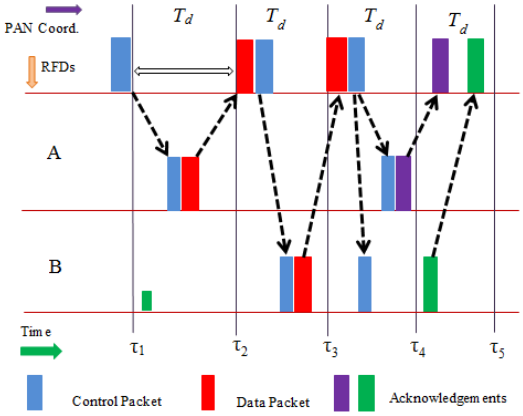

Fig. 3. The timing diagram of data transmission and reception in AR-MAC.

In this paper an attempt has been made to palliate the sink neighbourhood problem by avoiding the use of relay nodes/full function devices (FFDs) to forward the data from sensor nodes (RFDs). It is achieved by using only sensor nodes (RFDs) for the deployment of UWSNs and adjusting the speed of the mobile sink such that it will collect data from all the sensor nodes without the requirement of any sojourn. Moreover, the duty cycle of the sensor nodes is minimized as they become active only when the sink node reaches within their transmission range. Otherwise, they are in sleep mode, which reduces energy consumption, minimizes collisions, diminishes packets dropped and eliminates bottlenecks formation at the sink nodes. In recent research, there are several bottleneck constraints on exploiting the mobility of a sink for the enhancement of network performance. These constrictions include the maximum distance between two consecutive movements, the maximum number of sojourn locations and the minimum sojourn time at each sojourn location referred as the distance-constrained mobile sink problem is dulled by controlling the mobility and by

finding the most suitable path for the sink node to traverse the sensor network. The mobility of a sink node is a benediction to better balance the energy consumption among the sensors.

4. Preliminaries

The preliminaries are as follows:

- An underwater wireless sensor network *U(S, E)* is deployed comprising of *n* static sensors and a mobile sink, where *S* is the set of sensors and *E* is the set of radio links.
- There is no link between two static sensors as all the immobile sensors are reduced function devices (RFDs).
- The sink and a sensor node are able to communicate if they are within the communication range of each other.
- The energy consumed by all operations of communication is considered.
- It is assumed that by using radio positioning techniques the sink is aware of the location of the sensors.
- All sensors have the same data generation rate *r*.
- It is assumed that the mobile sink has limited energy which is sufficient for the completion of the monitoring operation in comparison with the energy capacity of sensors.
- There is no sojourn location of the mobile sink as it is continuously moving.

5. Mathematical Models

5.1. Underwater electromagnetic wave propagation

The conductivity, density and permittivity of water are different from and higher than air [17-18]. Water differs from the air as it has higher conductivity, higher density and higher permittivity. The value of relative permittivity of pure water is ε_r = 79, density is 1000 kg/m^3 and tangent loss is ε_t = 0.924 at 2.4 GHz. In the case of sea water ε_r = 80.4, density is 1033 kg/m^3 and ε_t = 1.527 at 2.4 GHz. The concentration of salt in the sea water determines the value of relative permittivity which is normally 3%. In this paper, the simulations are carried out for sea water only as the proposed protocol is meant for monitoring critical and real time data with minimized delay to perform underwater rescue operations in the sea successfully. The electromagnetic waves experience very high path loss in underwater propagation. Friis equation introducing the value of receiving power in the terms of transmitter and receiver antenna gains, transmitted power and path loss at the receiver is given in Eq. (1).

$$\Psi_r(dBm) = \Psi_i(dBm) + G_t(dBm) + G_r(dBm) - \Theta_{path}(dBm) \quad (1)$$

Where the gain of the transmitter and receiver antennas are denoted as G_t and G_r, the received power is Ψ_r, the transmitted power is Ψ_t and the underwater path loss is Θ_{path}. The expression for path loss is shown in Eq. (2).

$$\Theta_{path}(dB) = \Theta_o(dB) + \Theta_m(dB) + \Theta_a(dB) \tag{2}$$

The path loss in the air is denoted as Θ_o and formulated as expressed in Eq. (3).

$$\Theta_o(dB) = 20\log_{10}(\frac{4\pi df}{c}) \tag{3}$$

Where c is the velocity of electromagnetic waves in air in meter per second, the distance between transmitter and receiver in meters is denoted by d, the operating frequency in Hertz is symbolized as f. The path loss due to change in propagation medium is symbolised as Θ_m is expressed in Eq. (4).

$$\Theta_m = 20\log_{10}(\frac{\lambda_o}{\lambda}) \tag{4}$$

Where the wavelength of the signal in the air is signified as λ_0 and calculated as ($\lambda_0=c/f$), the wave factor λ is calculated as ($\lambda=2\pi/\beta$) and the phase shifting constant is denoted as β. Its value can be expressed as shown in Eq. (5).

$$\beta = \omega\sqrt{\frac{\mu\varepsilon}{2}}\left[\sqrt{1+(\frac{\sigma}{\omega\varepsilon})^2}\right]+1 \tag{5}$$

Where ω is the angular frequency in radians per second, σ is conductivity in Siemens per meter and μ is permeability in Henries per meter. The path loss due to attenuation in medium Θ_a is expressed in Eq. (6).

$$\Theta_a(dB) = 10\log_{10}(e^{-2\alpha d}) \tag{6}$$

Where the attenuation constant is denoted by α. Its value can be calculated as expressed in Eq. (7).

$$\alpha = \omega\sqrt{\frac{\mu\varepsilon}{2}}\left[\sqrt{1+(\frac{\sigma}{\omega\varepsilon})^2}\right]-1 \tag{7}$$

The parameters like propagation speed of EM wave v and the absorption coefficient ϑ are also very important. The expressions of these parameters are shown in Eqs. (8) and(9) respectively.

$$v \approx \frac{1}{\sqrt{(1+\chi_e)\times 8.85\times 10^{-12}\times\mu_r\times 4\pi\times 10^{-7}}} \tag{8}$$

$$\vartheta \approx \frac{\sigma}{2}\times\sqrt{\frac{\mu_r\times 4\pi\times 10^{-7}}{(1+\chi_e)\times 8.85\times 10^{-12}}} \tag{9}$$

Where ε_o, μ_o and χ_e are the permittivity, permeability of free space and electric susceptibility of sea water respectively. The relative permittivity and permeability of sea water are denoted by ε_r and μ_r respectively.

5.2. Calculation of reflection loss of water boundaries

The reflection is caused by the boundaries of water bodies such as water-air and water-sand interfaces [18] as shown in Fig. 4. The value of the reflection coefficient, Γ can be expressed as given by Eq. (10).

$$\Gamma = \frac{\rho_2 v_2 - \rho_1 v_1}{\rho_2 v_2 + \rho_1 v_1} \tag{10}$$

Where the density of water is denoted as ρ_1 and of other medium is signified as ρ_2. The wave velocity in water is denoted as v_1 and in another medium as v_2. The reflection loss from the surface and from the bottom is Θ_{ref} expressed in Eq. (11).

$$\Theta_{ref} = -V(dB) = -10\log_{10}(V) \tag{11}$$

Where V is calculated as shown in Eq. (12).

$$V^2 = 1 + (|\Gamma| e^{-\alpha\Delta(r)})^2 - 2|\Gamma| e^{-\alpha\Delta(r)} \times \cos(\pi - (\phi - \frac{2\pi}{\lambda}\Delta(r))) \tag{12}$$

Where $\Delta(r)$ is the difference between r and d in meters, $|\Gamma|$ and ϕ are the amplitude and phase of the reflection coefficient respectively and r is the reflected path length in meters. The expression to calculate r is shown in Eq. (13).

$$r = 2\sqrt{H^2 + (\frac{d}{2})^2} \tag{13}$$

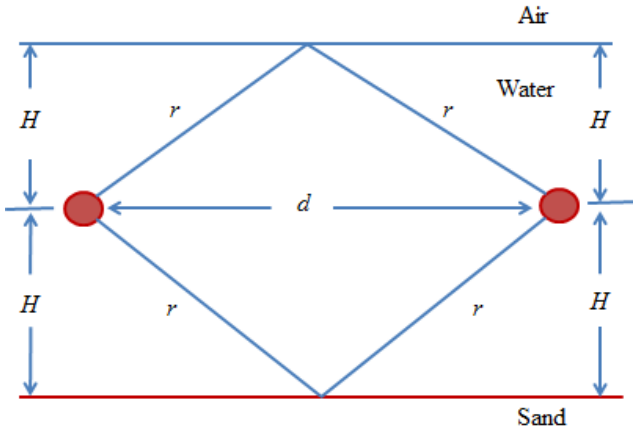

Fig. 4. A diagram representing three-path reflection model.

5.3. Calculation of throughput and delay

The maximum value of the throughput is directly proportional to the payload bytes and inversely proportional to the delay experienced by each data packet [19]. The superframe structure of IEEE 802.15.4 is shown in Fig. 5. The precise calculation of the delay and the determination of number of payload bytes are very important to exactly calculate the maximum throughput. The total delay comprises of the delay in data reception and the delay due to various frame sequences as shown in Fig. 6. Subsequently, the throughput (ρ) can be formulated as shown in Eq. (14).

$$\rho = \frac{8 \times \varphi}{\delta(\varphi)} \tag{14}$$

where φ denotes the payload bytes received from the network layer as shown in Fig. 7. The delay $\delta(\varphi)$ experienced by each packet can be expressed as shown in Eq. (15).

$$\delta(\varphi) = \tau_{BO} + \tau_{frame}(\varphi) + \tau_{TA} + \tau_{ACK} + \tau_{IFS}(\varphi) \tag{15}$$

where the symbols used and their meanings are mentioned below:

τ_{BO} = Back off period in seconds

$\tau_{frame}(\varphi)$ = Transmission time for a payload of φ bytes in seconds

τ_{TA} = Turnaround time in seconds

τ_{ACK} = Transmission time for an ACK in seconds

$\tau_{IFS}(\varphi)$ = Inter Frame Space time in seconds

κ = Payload size in bytes

If the size of the MAC Protocol Data Unit (MPDU) is smaller than or equal to 18 bytes than short inter frame space (SIFS) is used for the inter frame space (IFS). Otherwise, long inter frame space (LIFS) is used. The expression of MAC Protocol Data Unit (λ) is given in Eq. (16).

$$\lambda = \phi + \mu + \kappa \tag{16}$$

To calculate the total delay, it is important to calculate the time duration of its all components. The expression on the back off period is given in Eq. (17).

$$\tau_{BO} = \alpha \times \beta \tag{17}$$

where α is the number of back off slots and β is time for a back off slot.

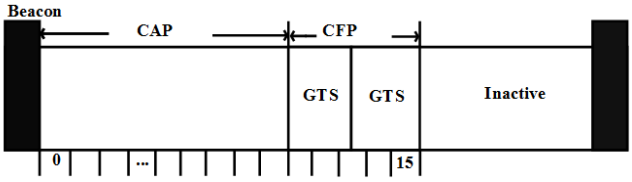

Fig. 5. The structure of the superframe in IEEE 802.15.4.

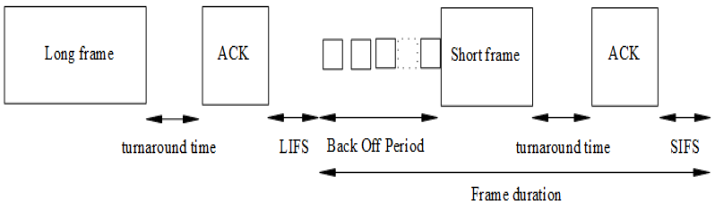

Fig. 6. The sequence of the frames of IEEE 802.15.4.

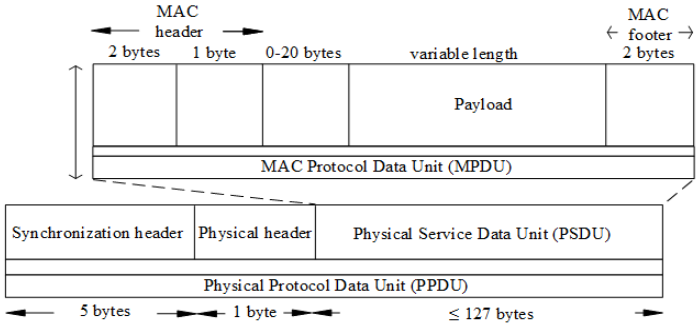

Fig. 7. The structures of the frames of IEEE 802.15.4.

The range of back off slots lies in the interval (0, 2^{BE}-1) where BE means the *back off exponent* having a minimum value of 3. As, the communication channel is assumed as perfect the value of BE will remain same. Therefore, the mean of the interval gives the number of back off slots which are: (2^{BE}-1)/2 or 3.5. The total duration of the frame in seconds is illustrated in Eq. (18).

$$\tau_{frame}(\varphi) = \frac{\psi + \phi + \Phi + \varphi + \mu}{\omega} \tag{18}$$

where ψ = Length of the PHY header is 6 bytes, ϕ = Length of the MAC header is 3 bytes, Φ = Length of the information field of MAC address in bytes, μ= Length of the MAC footer is 2 bytes, ω = Raw data rate in bits per second.

Equation (19) formulates the duration of an acknowledgement.

$$\tau_{ACK}(\varphi) = 8 \times \frac{\psi + \phi + \mu}{\omega} \tag{19}$$

The values of acknowledgement and turnaround times in seconds are equal to 0, if acknowledgements are not used. Finally, the mathematical formulation of the throughput (ρ) in bits per second is expressed in Eq. (20) and for the delay $\delta(\varphi)$ in seconds is in Eq. (21).

$$\rho = \frac{8 \times \varphi}{m \times \varphi + n} \tag{20}$$

$$\delta(\varphi) = m \times \varphi + n \tag{21}$$

In the above equations, the values of *m* and *n* are influenced by the operating frequency of the channel, length of data bytes in the payload (LISF or SIFS) and the length of the address. The values of parameters *m* and *n* are determined by using the curve fitting method considering the principle of least squares and by solving the respective normal equations to get the line of best fit.

5.4. Calculation of jitter

To calculate jitter [20], let us assume the UWSN as a set *M* consists of *n* nodes, $M = \{M_1, M_2, M_3 \ldots M_n\}$. Since each node periodically sends current status to the personal area network (PAN) coordinator or receives commands from it, we consider a set Γ composed of *n* periodic tasks. Every task $\Gamma_j = (R_j, D_j, T_j) \in \Gamma$ is

characterized by required number of time slots R_j, a relative deadline D_j and a period inter arrival time T_j. The effective scheduling of tasks using adaptive active/sleep cycles is very important to reduce jitter. In order to avoid deadline missing and improve the schedulability, the tasks are prioritized by various schedulers used. Consider a task Γ_j is scheduled at time slot *s*, the priority of this task P_j is calculated as expressed in Eq. (22).

$$P_j = D_j - s - T_j \tag{22}$$

5.5. Calculation of packets dropped

In this paper, Poisson process is implemented for the generation of packets at each sensor with parameter λ [21]. The exponentially distributed service times with parameter μ depends on the conduct of MAC protocols, and the influence of channel contention from other sensors. For the successful transmission of a packet, it should get completed within *d* time units after its arrival at the queue. For example, if a packet reaches at time *t*, it must get transmitted before its universal deadline ($t + d$), where *d* being a fixed relative deadline. The probability of successful packet transmission of the system is denoted as *PD(θ)* and its value is computed, where the threshold of packet dropping in seconds is denoted by θ. The number of packets present in the system, including the packets present in the transmitter immediately before a packet arrival is denoted by *X*. There are three states of a system experienced by a packet arriving in the system. These are empty, busy transmitter and full. The meaning of these states is explained as follows:

- *Empty (X = 0)*: The transmitter is available, and the buffer is also empty.
- *Busy Transmitter (X = 1)*: The transmission of a packet is in progress but the buffer is empty.
- *Full (X = 2)*: The transmission is in progress and the buffer is also full. In that case the reaching packet overwrote the packet already buffered.

The value of *PD(θ)* can be calculated in accordance with a condition, whether a packet reaches at an empty state or not. The service time experienced by the arriving packet is denoted by *Q*. The expression of *PD(θ)* is shown in Eq. (23).

$$PD(\theta) = \Pi(X = 0)\Pi(Q \le d) + (1 - \Pi(X = 0) \int_0^{d-\theta} \mu e^{-\mu t} \Pi(Q \le d - t) e^{-\lambda t} dt) \tag{23}$$

It can be justified as follows: The transmission of an arbitrary packet Π which arrives at an empty system can be successful only if the required time *Q* is less than *d*. This explains the term $\Pi(X = 0)\Pi(Q \le d)$. If Π arrives when the system is busy in transmitting a packet (X= 1 or X= 2), the beginning of its transmission depends on the remaining transmission time *t* of the packet that is presently being transmitted. The density of the remaining service time is exponentially distributed as $\mu e^{-\mu t}$. It is important to understand that these three conditions must be satisfied for the timely service of Π. First, the time of deadline is larger than θ when the remaining service ends, i.e., $d - t \ge \theta$.

Second, it is explained by the factor $\Pi(Q \le d-t)$, which means that the service time is less than $(t-d)$. Third, the term $e^{-\lambda t}$ explains it as there were no other arrivals during *t* time units. The schematic representation of data packets arriving and servicing is shown in Fig. 8.

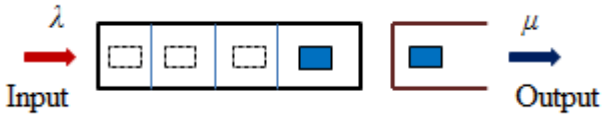

Fig. 8. The schematic representation of a queue.

5.6. The mathematical model of AR-MAC protocol

Describing *f(t)* as the transmitted signal sent from sensor node *g* to *h*. The mathematical expression of the transmitted signal is shown in Eq. (24) [22].

$$f(t) = f(t+T_o) \tag{24}$$

Where T_o denotes the time duration of the signal. The received signal at sensor node *h* is defined as shown in Eq. (25) [22].

$$z(t) = e^{-j2\pi\frac{\varphi}{1+\varphi}f_c T_o} z(t+\frac{T_o}{1+\varphi}) \tag{25}$$

Where φ is the Doppler scaling factor due to the relative velocity between sensor nodes and the mobile sink, and the clock skew is denoted as δ. The summation of the signals arrived along multiple physical paths is the received signal at the sink node can be formulated as shown in Eq. (26) [22].

$$Q_{hg}(t) = \sum_{k=1}^{N_k} A_k f_{gh}((1+\varphi_m)t - \tau_k) \tag{26}$$

Where $f_{gh}(t)$ is a transmitted message from sensor node *g* to *h* , with node g as the reference node. τ_k and A_k denote the delay and amplitude of the k^{th} path respectively. N_k signifies the number of paths. The joint Doppler scaling factor induced by the node mobility is thus $\varphi_m \cong \nu/\sigma$ where σ is the speed of electromagnetic waves in water and *v* is the relative velocity. The relative velocity of the two sensor nodes based on the joint Doppler scaling factor φ_m can be directly obtained as given in Eq. (27) [22].

$$\nu \cong \varphi_m \sigma = ((1+\varphi_{gh})\phi - 1)\sigma \tag{27}$$

ϕ signifies clock skew and φ_{gh} is Doppler scaling factor for sensors *g* and *h*. Finally, the propagation delay can be formulated as shown in Eq. (28) [22].

$$\tau = \frac{\delta\sigma - \phi t_r(\sigma + \vartheta) - \mu}{2\phi\sigma} \tag{28}$$

where ϑ is the velocity of the mobile sink in m/s, $t_r = (t_3 - t_2)$ and $\delta = (t_4 - t_1)$ as t_1, t_2, t_3 and t_4 are different time instants, $\mu = 1/2\alpha t_r^2$ as α denotes acceleration of the mobile sink node. Let *v* is the velocity of the mobile sink and D_{ij} is the path length in meters from location *i* to *j* during which the sensor nodes from S_i to S_j are active is formulated as shown in Eq. (29).

$$D_{ij} = v(\tau_j - \tau_i) \forall i, j \tag{29}$$

The sensors are having different *ON/OFF* time periods depending on the location and velocity of the mobile sink. The sensor number S_i active during the i^{th} time slot τ_i is expressed as shown in Eq. (30)

$$\sum_{i}^{i+3} S_i = \tau_i \text{ where } i=1 \tag{30}$$

$$\sum_{j}^{j+3} S_j = \tau_j \text{ where } j=i+3 \tag{31}$$

The expression for the n^{th} number of sensor can be expressed as given in Eq. (32).

$$\sum_{n}^{n+3} S_n = \tau_n \text{ where } n=j+3 \tag{32}$$

The total simulation time T_{sim} is equal to 670 seconds for 100 nodes and 1395 seconds for the 200 nodes. It is formulated as shown in Eq. (33).

$$T_{sim} = \overset{\tau_1}{\underset{0}{T_1}} + \overset{\tau_2}{\underset{\tau_1+1}{T_2}} + \ldots\ldots + \overset{\tau_n}{\underset{\tau_{n-1}}{T_n}} \tag{33}$$

The duty cycle of each and every sensor node (RFD) is adjusted by varying the ON/OFF time. In the proposed scenario a sensor node is active for 28 seconds, which means that for the network of 100 nodes having total simulation time of 670 seconds, duty cycle is about 4.1%. Likewise, for the network of 200 nodes having total simulation time of 1395 seconds, duty cycle is about 2%. The aim of the proposed AR-MAC is the minimum average end to end delay, minimum jitter as well as improved other performance metrics. The aim to achieve a minimum average end to end delay is expressed in Eq. (34).

$$aim = \min \delta(\varphi) \tag{34}$$

6. Simulation Scenario and Algorithms

6.1. General scenario of UWSNs

Figure 9 shows the general scenario of UWSNs consisting of different types of sensor nodes and autonomous underwater vehicles used for collaborative monitoring. The underwater sensors are linked with each other via microwave links. Further, the surface sink nodes are connected to the control center via radio frequency links. The architectures are application dependent, either 3-dimensional or 2-dimensional. The ordinary sensor nodes sense and relay data using direct link or through a multi-hop path. The mobility of sensor nodes as well as sink nodes can be classified as controlled mobility and uncontrolled mobility. This paper implements radio links for both underwater and free space communication. The sensed data are transmitted through direct radio links and the mobility of the sink node is controlled.

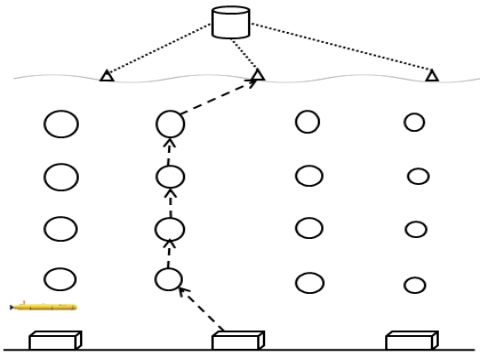

Fig. 9. General Scenario of UWSN.

Legends used in Fig. 9.

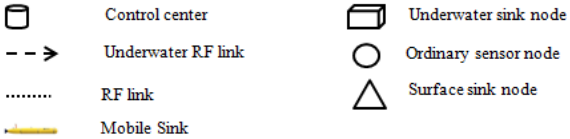

6.2. Lawn-mower trajectory for the mobile sink

The lawn-mower trajectory of the mobile sink as shown in Fig. 10 is considered after extensive simulations to reduce the requirement of multi-hop data transmissions. As the network, constitutes of all RFDs except the mobile sink to avoid multi-hop data transmissions to reduce the depletion of battery power. This trajectory is most suitable as the sink node is available for all sensors within their transmission range after regular interval of times, but at the cost of increased path length. The deteriorating effect of the increased path length is reduced by implementing effective path determination (EPD) algorithm. The velocity of the sink node is selected so that each and every sensor node gets sufficient time to synchronize and to transmit the sensed data without the requirement of any sojourns.

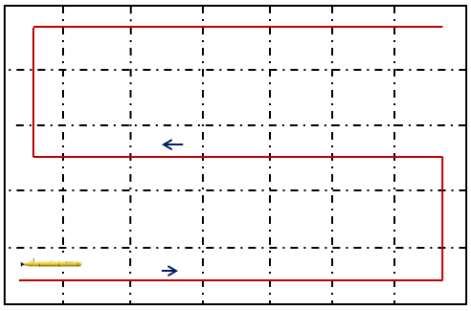

Fig. 10. The representation of Lawn-mower trajectory of the mobile sink.

6.3. Determination of data rate

The expression of transmission data rate r of data sent to sensor q denoted by r_q [23] can be written as shown in Eq. (35).

$$r_q = B\log_2(1+\frac{P_q g_q(x^*, y^*)}{\sum_{m=q+1}^{n} P_m h_q(x^*, y^*) + N_0}) = l_q K_r^* \tag{35}$$

Where B is the available bandwidth, P_q is the power assigned to transmission to sensor q, $g_q(x^*, y^*)$ is the channel gain as a function of the distance, K_r^* is the ratio of rate of transmissions to the message length, l_q is the length of the message sent to sensor q and N_0 is the expected ambient noise. To attain the transmission power P_i in the terms of x^*, y^* and K_r^*, Eq. (35) can be recursively solved to get the expression given in Eq. (36).

$$P_i(x^*, y^*, K_r^*) = (2^{l_q K_r^*} - 1) \times \frac{(N_0 + \sum_{m=q+1}^{n} P_m(x^*, y^*, K_r^*) h_q(x^*, y^*))}{h_q(x^*, y^*)} \tag{36}$$

Equation (36) illustrates the influence of all prime parameters on the power allotted to the transmission to sensor i. To determine effective path length and optimum throughput path, the sink needs to evaluate the maximum K_r possible over the entire network and then select the position with the highest K_r.

6.4. Path designing

This section describes two algorithms. Algorithm 1 is proposed to find out the effective path length and Algorithm 2 to determine the maximum throughput path for the mobile sink. It is assumed that the sensors are properly anchored to limit their movement due to waves within the permissible limits to follow these algorithms.

Algorithm 1	**Effective Path Length Determination (EPD)**
STATE:	The initial position of the mobile sink.
The initial position is P on the water surface. Let the desired position is $\mathcal{P}$.	
	while $P \neq \mathcal{P}$ do
	$P = \mathcal{P}$
STATE:	Connections using radio Channel
Initialize the maximum range = r_{max}.	
The location of the sensor k is L_k.	
The total number of sensors in the network are N.	
The point of the present position of the sensor k is L_k^m and the distance between the sink and sensor node k is $D_{k,m}$.	
	$D_{k,m} = \| L_k^m - P \|, \forall L_k^m \in P$.
	if $D_{k,m} \leq r_{max}$ then
	Path found; break.
	end if
STATE:	Re-evaluate Effective Path and Reallocate Sensors
Find P that minimizes max $\| L_k^m - P \| \ \forall \ P \in L_k^m$.	
	If $P = \mathcal{P}$ and $D_{k,m} > r_{max}$ for any m then
	No path found; break.
	end if
	end while
STATE:	Location Modification
Solve the equation (36) to attain the optimal location to achieve the maximum K_r for the sink node.	

Algorithm 2	**Optimum Throughput Path Determination (OTPD)**
Initialize:	Number of segments S = 1; iteration time q = N; Set segment(k) = 1 ∀ k
Generate $n \times n$ distance matrix X and calculate throughput $\mathcal{T}$.	
	While q> 0 do
	Find the reference throughput $\mathcal{T}$ at distance r_{max} = 20 m.
	if $\mathcal{T}_{new} \geq \mathcal{T}$ then
Optimum throughput path found. Delete entries in X corresponding to k.	
	$S = S+1$; $q = q+1$
	end if
	end while
STATE:	Re-calculate optimum throughput path
	while q > 0 do
	if $\mathcal{T}_{new} < \mathcal{T}$ then
Optimum throughput path not found.	
	end if
	end while
Solve the equation (36) to attain the optimal location to achieve the maximum K_r for the sink node.	

6.5. Queues and Schedulers

The network scenario presented in this paper has implemented different queue types as First-In First-Out (FIFO), Randomly Early Detection (RED), Random Early Detection with I/O bit and Weighted Random Early Detection. Each of them is implemented with different queue sizes in bytes such as 20000, 22000, 25000, 26000, 27000, 30000, 50000, 150000, 200000, 250000, 500000 and 1000000. The schedulers employed are Differentiated services weighted fair, Round Robin and Self-clocked fair. The intent is to effectively schedule the transmission and reception of data packets.

7. Simulation Results and Analysis

In this section, we present simulation results to evaluate the performance of the proposed AR-MAC to minimize average end to end delay without degrading other performance parameters and compare it with IEEE 802.15.4 protocol. The simulation parameters are shown in Table 1 and the simulations are performed using Qualnet 6.1 simulator. The ten rounds of simulation are performed and their average value is considered for more accurate results.

7.1. Sequence of steps followed in simulation

The flow chart demonstrating the steps followed in the simulation is shown in Fig. 11. The evaluation and comparison of throughput as a performance parameter for the different types of queues and schedulers at different queue sizes is presented in Figs. 12 and 13.

Table 1. The simulation parameters.

S. No.	Parameter(s)	Value(s)
1.	Total number of nodes	101, 201
2.	Number of PAN coordinator	1, 1
3.	Number of RFDs	100, 200
4.	Communication Protocols RFDs to PAN coordinator PAN to RFDs	 IEEE 802.15.4 IEEE 802.15.4
5.	Channel frequency (GHz)	2.4
6.	Packet size (bytes)	38
7.	Packet interval (secs)	1
8.	Simulation Times (secs)	670, 1395
9.	Battery (mAh)	1200
10.	Transmission range (m)	20
11.	Nodes connectivity RFDs to PAN PAN to RFDs	Protocol, Frequency (GHz) ZigBee, 2.4 ZigBee, 2.4
12.	Terrain Area (m^2)	$110\times20\times110$, $210\times20\times110$
13.	Energy Model	Mica-motes
14.	Battery model	Linear
15.	Optimum queue size (bytes)	26000
16.	Queue type	Random Early Detection
17.	Scheduler type	Round Robin
18.	Application	Traffic-Generator
19.	Speed of PAN (m/s)	0.7164

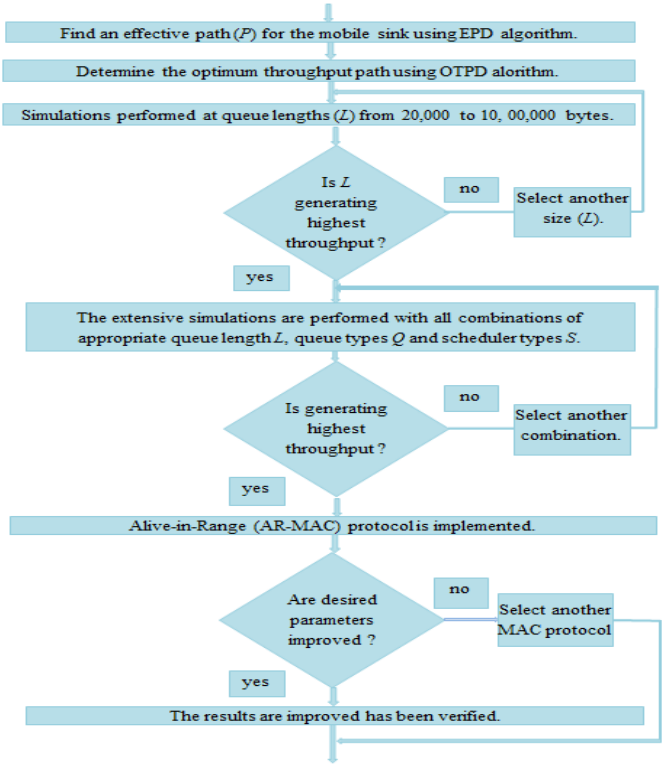

Fig. 11. The flow chart of the proposed model.

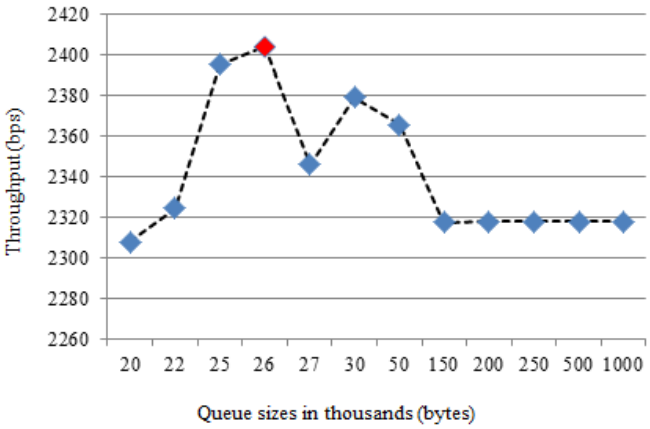

Fig. 12. The Performance evaluation at different queue sizes.

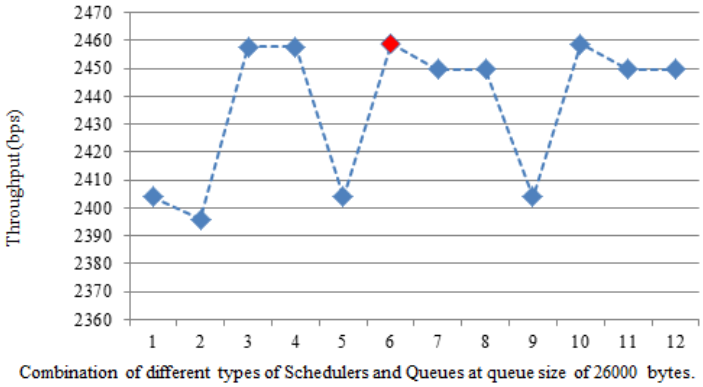

Fig. 13. The Performance evaluation using different schedulers and queues of 26000 bytes.

Legends used in Fig. 13:
Number – Scheduler/Queue

1 – Differentiated service weighted fair/First-in first-out
2 – Differentiated service weighted fair/Random early detection
3 – Differentiated service weighted fair/Random early detection with I/O bit
4 – Differentiated service weighted fair/Weighted Random early detection
5 – Round robin/ First-in first-out
6 – Round robin/ Random early detection
7 – Round robin/ Random early detection with I/O bit
8 – Round robin/ Weighted Random early detection
9 – Self-clocked fair/ First-in first-out
10 – Self-clocked fair/ Random early detection
11 – Self-clocked fair/ Random early detection with I/O bit
12 – Self-clocked fair/ Weighted Random early detection

7.2. Throughput

Figure 14 illustrates how throughput has improved after the implementation of effective path determination, optimum throughput path determination algorithm.

The selection of appropriate queue length, suitable type of schedulers and queues is also responsible for the successful reception of data bits. The implementation of AR-MAC has increased synchronization among nodes and reduced the collisions during contention access period significantly, which leads to the enhancement of throughput commendable for the better quality of the received data.

7.3. Average end to end delay

The main objective of this work to reduce average end to end delay in the underwater wireless sensor network is achieved as presented in Fig. 15. It is reduced significantly due to the selection of suitable queues and schedulers to the appropriate queue size. The utilization of efficient algorithms and the protocol to improve the synchronization between sensors by implementing active/sleep cycles precisely play very important role in the reduction of delay. It is desirable that in-spite of increasing the number of nodes the delay is still low.

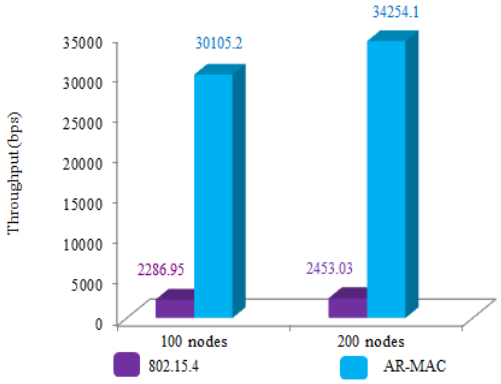

Fig. 14. Throughput (bps).

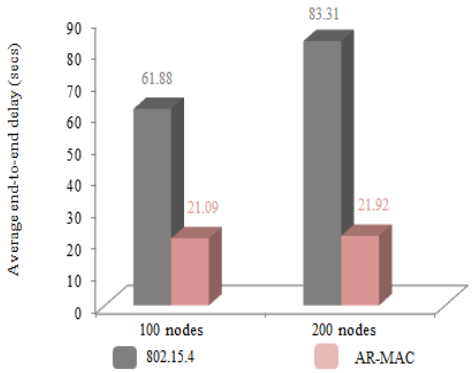

Fig. 15. Average end to end delay (secs).

7.4. Jitter

Figure 16 demonstrates the encouraging influence of the proposed protocol on jitter. For crucial and real time data monitoring jitter should be very low to minimize the

delay between the expected and actual time of data reception at the sink node. The proposed algorithms and the protocol reduce the jitter significantly.

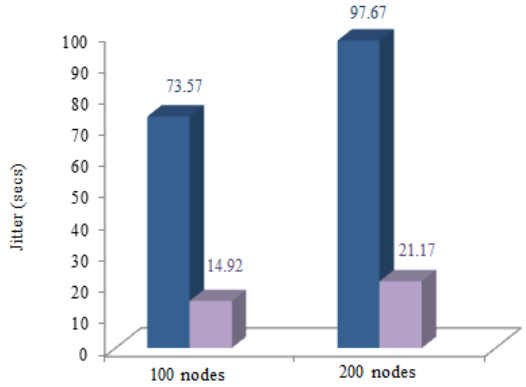

Fig. 16. Jitter (secs).

7.5. Total number of packets dropped

Figure 17 compares the total number of packets dropped in networks of 100 and 200 nodes, between IEEE 802.15.4 and the proposed AR-MAC protocol. The selection of apt queue size, types of queues and schedulers with precise ON/OFF timings and the duration of active period are liable for the convincing reduction in the number of packets dropped.

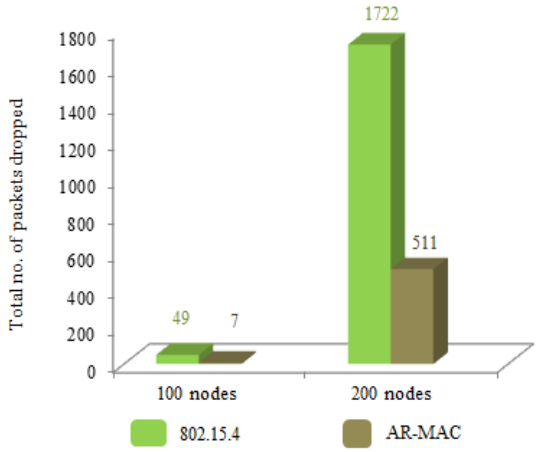

Fig. 17. Packets dropped.

7.6. Network lifetime

Figure 18 evaluates the influence of AR-MAC protocol on the lifetime of the network. The results clearly signify that along-with the improvement in throughput, reduction in delay, jitter and the number of packets dropped, it also prolongs the network lifetime to some extent. It is due to the implementation of

proficient algorithms and AR-MAC protocol which enhance the synchronization between nodes by implementing duty cycles effectively.

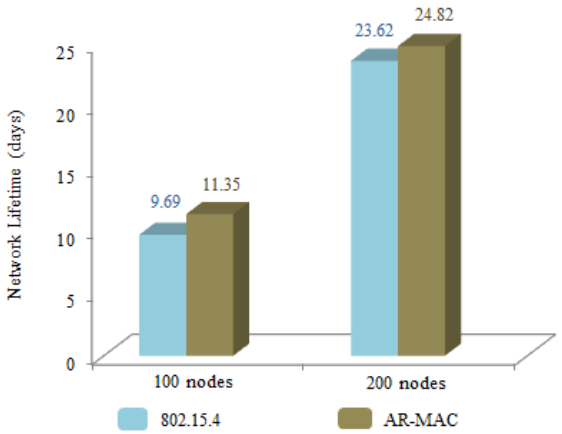

Fig. 18. Network Lifetime.

8. Conclusion and Future Work

In this paper, we have presented AR-MAC protocol implemented with effective path and optimum throughput path determination algorithms after the determination of apt queue size, queue type and scheduler type. The aim to minimize average end to end delay has been successfully achieved along-with the improvement in other performance metrics. Simulation results validate our protocol under various application requirements and network conditions.

In the future, we intend to resolve the influence of clock skew and sensor mobility in underwater sensor networks.

References

1. Akyildiz, I.F.; Pompili, D.; and Melodia, T. (2005). Underwater acoustic sensor networks: research challenges. *Ad Hoc Networks*, 3(3), 257-279.
2. Akyildiz, I.F.; Pompili, D.; and Melodia, T. (2007). State of the art in protocol research in underwater acoustic sensor networks. *ACM Mobile Computing Communications Review*, 11(4), 11-22.
3. Weifa, L.; Jun, L.; and Xu, X. (2010). Prolonging Network Lifetime via A Controlled Mobile Sink in Wireless Sensor Networks. *IEEE Proceedings of Global Telecommunications Conference*, Miami, Florida, USA, 1-6.
4. Ayaz, M.; Baig, I.; Abdullah, A.; and Faye, I. (2011). A survey on routing techniques in underwater wireless sensor networks. *Journal of Network and Computer Applications*, 34(6), 1908- 1927.
5. Francesco, M.D.; Das, S.K.; and Anastasi, G. (2011). Data collection in wireless sensor networks with mobile elements: A survey. *ACM Transactions on Sensor Networks*, 8(1), 1-31.

6. Rahim, M.S.; Casari, P.; Guerra, F.; and Zorzi, M. (2011). On the performance of delay-tolerant routing protocols in underwater networks. P*roceedings of the IEEE*, 1(1), 1-7.
7. Yoon, S.; Azad, A.K.; Oh, H.; and Kim, S. (2012). AURP: An AUV-aided underwater routing protocol for underwater acoustic sensor networks. *Sensors*, 12(2), 1827-1845.
8. Hollinger, G.A.; Choudhary, S.; and Qarabaqi, P. (2012). Underwater data collection using robotic sensor networks. *IEEE Journal on Selected Areas in Communications*, 30(5), 899-911.
9. Motoyama, S. (2012). Flexible polling-based scheduling with QoS capability for wireless body sensor network. *IEEE Proceedings of the 37th Conference on Local Computer Networks Workshops*, Clearwater, Florida, USA, 745-752.
10. Konstantopoulos, C.; Pantziou, G.; Gavalas, D.; Mpitziopoulos, A.; and Mamalis, B. (2012). A rendezvous-based approach enabling energy-efficient sensory data collection with mobile Sinks. *IEEE Transactions on Parallel and Distributed Systems*, 23(5), 809-817.
11. Favaro, F.; Casari, P.; Guerra, F.; and Zorzi, M. (2012). Data upload from a static underwater network to an AUV: polling or random access? *Proceedings of OCEANS*, 1(1), 1-6.
12. Favaro, F.; Brolo, L.; Toso, G.; Casari, P.; and Zorzi, M. (2013). A study on remote data retrieval strategies in underwater acoustic networks. *Proceedings of MTS/IEEE OCEANS Conference*, Bergen, 1-8.
13. Roy, S.; Shome, S.N.; Nandy, S.; Ray, R.; and Kumar, V. (2013). Trajectory following control of AUV: a robust approach. *Journal The Institution of Engineers (India): Series C*, 94(3), 253- 265.
14. Rahman, R.H.; and Frater, M.R. (2014). Delay-tolerant networks (DTNs) for underwater communication. *Advances in Delay Tolerant Networks: Architecture and Enhanced Performance*, *Elsevier*,1(1), 81-103.
15. Jalaja, M.J.; and Jacob, L. (2014). On-demand data collection in sparse underwater acoustic sensor networks using mobile elements. *Proceedings of the 10th International Conference on Wireless and Mobile Communication*, Seville, Spain, 105-111.
16. Jalaja, J.K.; and Lillykutty, J. (2015). Delay and Lifetime Performance of Underwater Wireless Sensor Networks with Mobile Element Based Data Collection. *International Journal of Distributed Sensor Networks*, 8(1), 1-22.
17. Sendra, S.; Lloret, J.; Rodrigues, J.J.P.C.; and Aguiar, J.M. (2013). Underwater Wireless Communications in Freshwater at 2.4 GHz. *IEEE Communication Letters*, 17(9), 1794-1797.
18. Ali, E.; Abdelrahman, E.; Majed, A.; and Khaled, E. (2012). Underwater Wireless Sensor Network Communication using Electromagnetic Waves at Resonance Frequency 2.4 GHz. *Proceedings of the 15th Communication and Networking Simulation Symposium*, Orlando, Florida, USA, 1-7.
19. Latré, B.; Mil, P.D.; Moerman, I.; Dhoed, B.; and Demeester, P. (2006). Throughput and Delay Analysis of Unslotted IEEE 802.15.4. *Journal of Networks*, 1(1), 20-28.

20. Yu, K.; Gidlind, M.; Akerberg, J.; and Bjorkman, M. (2013). Low Jitter Scheduling for Industrial Wireless Sensor and Actuator Networks. *IEEE Proceedings of the 39th Annual Conference of the Industrial Electronics Society*. Sweden, 5594-5599.
21. Aoun, M.; and Argyriou, A. (2012). Queueing Model and Optimization of Packet Dropping in Real-Time Wireless Sensor Networks. *IEEE Proceedings of the Communications QoS, Reliability and Modelling Symposium*, Ottawa, Canada, 1687-1691.
22. Liu, J.; Wang, Z.; Zuba, M.; Peng, Z.; Cui, J.H.; and Zhou, S. (2014). DA-Sync: A Doppler-Assisted Time Synchronization Scheme for Mobile Underwater Sensor Networks. *IEEE Transactions on Mobile Computing*, 13(3), 582-595.
23. Yang, H.; and Sikdar, B. (2008). A mobility based architecture for underwater acoustic sensor networks. *IEEE Proceedings of Global Telecommunications Conference*, New Orleans, LA, USA, 1- 5.